

# Impact of O–Si–O bond angle fluctuations on the Si–O bond-breakage rate

Stanislav Tyaginov<sup>a,\*</sup>, Viktor Sverdlov<sup>b</sup>, Ivan Starkov<sup>a</sup>, Wolfgang Gös<sup>a</sup>, Tibor Grasser<sup>a</sup>

<sup>a</sup> Christian Doppler Laboratory for TCAD, Technische Universität Wien, Gußhausstraße 27–29/E 360, A-1040 Vienna, Austria

<sup>b</sup> Institute for Microelectronics, Technische Universität Wien, Gußhausstraße 27–29/E 360, A-1040 Vienna, Austria

## ARTICLE INFO

### Article history:

Received 19 June 2009

Available online 7 August 2009

## ABSTRACT

We extend the McPherson model for the silicon–oxygen bond-breakage in a manner to capture the impact of the O–Si–O angle fluctuations (typical for amorphous SiO<sub>2</sub>) on the breakage rate. In the McPherson model the transition of the Si ion from the 4-fold coordinated position to the 3-fold coordination is considered as rupture of the Si–O bond. We have studied the potential barrier (separating these saddle points) transformation induced by the O–Si–O bond angle variations and found that the secondary minimum occurs at a critical angle of about 107.75°. Since the Si ion “finds” the way corresponding to the highest breakage probability we used the two-dimensional downhill simplex method in order to find the direction of this maximal rate. It was shown that if the O–Si–O angle deviates from its nominal value 109.48° (typical for  $\alpha$ -quartz) corresponding to the regular SiO<sub>4</sub> tetrahedron the symmetry aggravates and the secondary minimum is rotated. Calculated dependencies of the breakage rate on the electric field demonstrate the linear slope in the log–lin scale thus reflecting the linear reduction of the activation energy for the bond-breakage vs. field. The family of distribution functions for breakage rate calculated with a fixed step of field shows that the curves do not change their form and are shifted in parallel with the field. This tendency supports the thermo-chemical model for the bond-breakage also in the case of strongly fluctuating O–Si–O angles. As a consequence, dependencies of the mean value of the rate, its standard deviation and the nominal rate (calculated for the angle of 109.48°) have the same slope on a log–lin scale. The wide spread of the breakage rate is reflected by the high value of its standard deviation.

© 2009 Elsevier Ltd. All rights reserved.

## 1. Introduction

The Si–O bond-breakage has been suggested to be a crucial contributor to hot-carrier-injection (HCI) damage and to time-dependent-dielectric-breakdown (TDDB) [1,2]. A model recently proposed by McPherson [3,4] considers Si–O bond rupture as a transition of the Si ion from the 4-fold equilibrium position (the primary minimum) in the center of the SiO<sub>4</sub> tetrahedron to the 3-fold position (the secondary minimum/saddle point) beyond the O<sub>3</sub> plane (Fig. 1a), resulting in the formation of a Si–Si bridge. This transition is considered as a superposition of the Si ion tunneling through the barrier between the primary and the secondary minima and its thermionic excitation over this barrier. The potential profile is formed by four contributions due to interactions of the Si with the surrounding O ions situated in the vertices of the SiO<sub>4</sub> tetrahedron. To describe Si–O interactions the Mie–Grüneisen pair-wise interatomic potential has been used [3,4].

Although it has been speculated that the secondary minimum becomes more/less energetically pronounced with O–Si–O angle

$\varphi$  deviations and, thus the bond-breakage rate may be drastically changed, this issue has not been quantitatively addressed. At the same time there is a bulk of either theoretical [5–7] or experimental [8,9] publications where a distribution of O–Si–O and Si–O–Si angles is reported for amorphous SiO<sub>2</sub>. Therefore, the McPherson model is only suitable for  $\alpha$ -quartz and has to be extended in a way to capture the effect of fluctuations of these angles typical for SiO<sub>2</sub> films employed as gate oxides. We study the impact of O–Si–O angle variations on the breakage rate.

## 2. McPherson model: General considerations

As a starting point the McPherson model for Si–O bond-breakage is used [3,4]. We employ the Mie–Grüneisen interatomic potential to describe Si–O interactions:

$$\Phi(r) = \Phi_B \left[ A \left( \frac{r_0}{r} \right)^9 - B \left( \frac{r_0}{r} \right)^2 - C \left( \frac{r_0}{r} \right) \right] \quad (1)$$

where  $r$  is the interatomic distance,  $\Phi_B = 5.4$  eV and  $r_0 = 1.7$  Å are the bond strength and length. Constants  $\{A, B, C\}$  are found in order to satisfy the set of requirements:

\* Corresponding author. Tel.: +43 1 58801 36025; fax: +43 1 58801 36099.  
E-mail address: [tyaginov@iue.tuwien.ac.at](mailto:tyaginov@iue.tuwien.ac.at) (S. Tyaginov).

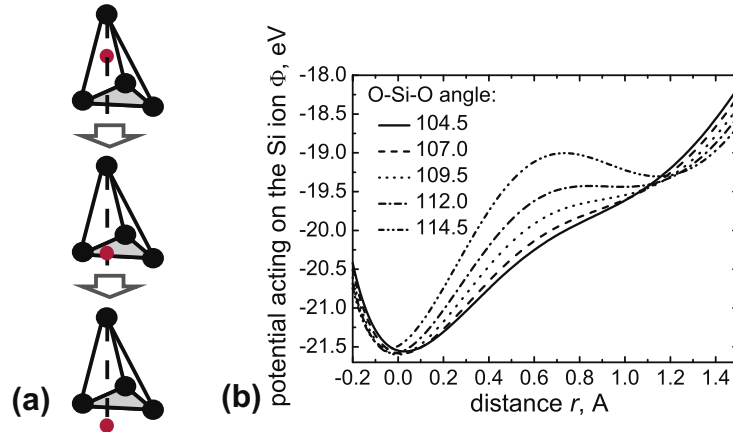


**Fig. 1.** Geometrical and energetical positions of the secondary minimum: (a) Si transition from the 4-fold to the 3-fold position and (b) barrier transformation with O–Si–O angle.

$$\Phi(r_0) = \Phi_B \quad (2a)$$

$$\left. \frac{\partial \Phi}{\partial r} \right|_{r=r_0} = 0 \quad (2b)$$

$$\frac{C}{B+C} = f_0^* \quad (2c)$$

Eqs. (2a) and (2b) represent the energetical and spatial position of the minimum corresponding to the equilibrium interatomic distance  $r = r_0$ , while (2c) ensures the suitable bond polarity  $f_0^* \cong 0.6$  (see [3] and its references).

In the McPherson model the position of the secondary saddle point is determined by the tetrahedral symmetry. The secondary minimum lies on the symmetry axis of the tetrahedron, i.e. in the direction from the center of the  $\text{SiO}_4$  cell perpendicular to the  $\text{O}_3$  plane (Fig. 1a). While moving the Si atom in this direction – due to the symmetry – the contributions of three oxygen ions in the plane are identical featuring a maximum when Si penetrates the plane and two minima situated symmetrically with respect to this maximum. The potential profile for the last Si–O bond demonstrates the unique minimum (cf. Eq. (1)) at the equilibrium ion distance shifted with respect to the  $\text{O}_3$  plane perpendicularly and, therefore, this last contribution deepens the primary minimum and flattens the secondary one, thus transforming it into a ledge. These minima are separated by the barrier originated from the contribution of the  $\text{O}_3$  plane forming the in-plane maximum (Fig. 1b).

### 3. McPherson model: Bond-breakage mechanisms

The breakage of the silicon–oxygen bond is treated as the superposition of two mechanisms, namely of the Si ion tunneling between two saddled positions accompanied by thermionic excitation over the potential barrier. Tunneling is treated quasi-classically within the Wentzel–Kramers–Brillouin (WKB) approximation. The system of energy levels in the quantum well of the primary minimum is found by numerically solving

$$\int_{x_1}^{x_2} \sqrt{2m_{\text{Si}}(E_n - V(x))} dx = (n + 1/2)\pi\hbar \quad (3)$$

where  $n$  and  $E_n$  are the level number and its position,  $V(x)$  is the potential profile,  $m_{\text{Si}}$  is the Si ion mass and the integration is performed over the classically allowed interval of the ion movement (restricted by points  $x_1$  and  $x_2$ ).

The Si ion “flux” from each level  $P_{tu,n}$  – which is actually the tunneling rate – is the product of the level occupancy (number of available particles), attempt frequency (reciprocal aller–retour

time  $\tau_{a-r,n}$ , i.e. the time between two consequent collisions with the potential profile) and the barrier transparency  $T_n$ , i.e.:

$$P_{tu,n} = \frac{f_n T_n}{\tau_{a-r,n}} \quad (4)$$

The level occupancy  $f_n$  obeys Boltzmann statistics:

$$f_n = \exp(-E_n/k_B T) / \sum_n \exp(-E_n/k_B T) \quad (5)$$

where the denominator (the statistical sum) warrants the normalization;  $k_B$  is the Boltzmann constant while  $T$  is the absolute temperature.

Having a certain ion energy  $E_n$  one may find reference points  $\{x_2, x_3\}$  limiting the classically prohibited region of movement while solving  $E_n = V(x)$  and then write the tunnel probability and the aller–retour time as [3,4,10]:

$$T_n = \exp\left(-\frac{2}{\hbar} \int_{x_2}^{x_3} \sqrt{2m_{\text{Si}}[V(x) - E_n]} dx\right) \quad (6)$$

$$\tau_{a-r,n} = 2\sqrt{\frac{m_{\text{Si}}}{2}} \int_{x_1}^{x_2} \frac{dx}{\sqrt{E_n - V(x)}} \quad (7)$$

Note that the total tunnel rate is to be found by summation over all states of the Si ion. Another important contribution to the bond-breakage process is related to the thermal excitation of the ion over the potential barrier characterized with the rate:

$$P_{th} = \nu \cdot \exp(-E_a/kT) \quad (8)$$

where  $E_a$  is the activation energy (difference in energetical positions of the primary minimum and the maximum separating these minima) and  $\nu = 10^{13} \text{ s}^{-1}$  is the attempt frequency [3,4].

While shifting one of O ions from its regular position corresponding to  $\alpha\text{-SiO}_2$  or, in other words, while deviating the O–Si–O angle, the symmetry is distorted and the position of a ledge is shifted both geometrically and energetically. With an increase of  $\varphi$  the saddle point becomes more pronounced and at the same time the barrier separating the primary and the secondary minima grows as depicted in Fig. 1b. This means that thermionic contribution decays with  $\varphi$  while it is not clear *a priori* how the tunnel component behaves. Since the Si ion tunnels from those levels in the quantum well of the primary minimum situated above the bottom of the secondary minimum, there is a trade-off between aggravation of the tunnel probability due to the higher barrier and its growth due to involvement of a larger number of levels into tunneling.

#### 4. Bond-breakage rate vs. O–Si–O bond angle

It is obvious that the direction in which the secondary minimum appears is determined by the  $\text{SiO}_4$  tetrahedron symmetry. Thus if one of the O ions is shifted ( $\varphi$  is not equal to its conventional value of  $109.48^\circ$  in crystalline  $\text{SiO}_2$ , see Fig. 2a) the minimum should be observed in another direction. However, we consider here the overall bond-breakage rate. In other words, a path between the primary and the secondary minima providing the highest rate will be “found” by the Si ion while breaking Si–O bond. Therefore, it is more reasonable to reformulate the problem in terms of “bond-breakage rate” rather than “potential profile”, i.e. to find the direction in which a maximum of bond-breakage rate  $P$  is observed.

Fig. 2b demonstrates the dependence of the modulus of angle  $\theta$  between the  $\text{SiO}_4$  symmetry axis and the direction corresponding the maximal of  $P$  as a function of  $\varphi$ . Note that this dependence features  $\theta = 0$  for  $\varphi = 109.48^\circ$  as it should be (the case of the regular  $\alpha$ -quartz). Let us assume that the O ion marked as 2 is moved toward the symmetry axis of the  $\text{SiO}_4$  cell ( $\varphi > 109.48^\circ$ ). It is obvious that in this case the direction corresponding the maximal rate  $P$  will be rotated towards other ions from the  $\text{O}_3$  plane. In other words, if we assign negative values of  $\theta$  for directions from the symmetry axis toward the O ion marked as 4, we have  $\theta < 0$  for  $\varphi > 109.48^\circ$ . Just the same qualitative findings lead us to  $\theta > 0$  for  $\varphi < 109.48^\circ$ . Fig. 2b confirms these considerations demonstrating the change of  $\theta$  sign while  $\varphi$  passes  $109.48^\circ$ .

To determine  $\theta$  we used the downhill simplex method in two dimensions (while searching the maximum we examined directions connecting the  $\text{SiO}_4$  center and a point in the  $\text{O}_3$  plane parameterized by two coordinates), see e.g. [11]. Note that only directions demonstrating a pronounced secondary minimum have been taken into account (a zero bond-breakage rate was assigned to a direction with no secondary minimum observed). Fig. 3 shows the dependence of  $P$  on  $\varphi$  calculated for different values of fields  $F$ . One can see an abrupt increase of  $P$  at  $\varphi_{cr} = 107.75^\circ$  corresponding to the appearance of the secondary minimum. The following decrease of bond-breakage rate with  $\varphi$  reflects the interplay between the barrier strengthening and deepening of the secondary minimum mentioned above. Note that the dependences  $P(\varphi)$  calculated with a certain step on  $F$  are situated equidistantly on a log–lin scale, meaning that the bond-breakage rate grows exponentially with field, supporting the thermo-chemical model for the silicon–oxygen bond-breakage [3,4,12] even for the case of fluctuating  $\varphi$ . The rate  $P$  as a function of  $F$  calculated for various values of  $\varphi$  is plotted in Fig. 4, explicitly demonstrating a linear trend for the logarithmic rate vs. the electric field. Note that all the curves  $P(F)$  have the same slope.

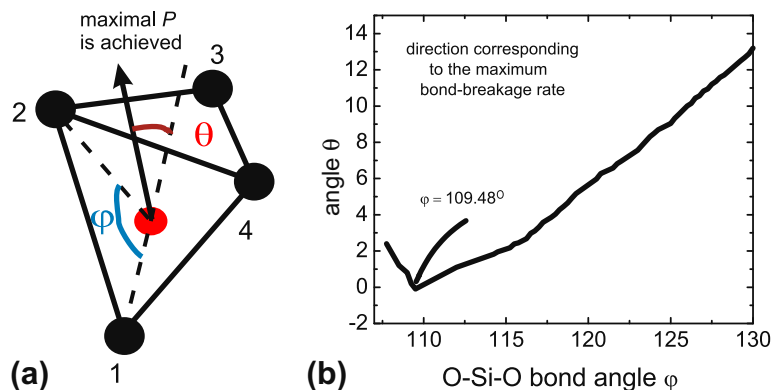


Fig. 2. Direction at which the maximum bond-breakage rate is observed (represented by angle  $\theta$ ): (a) schematically depicted and (b) as a function of angle  $\varphi$ .

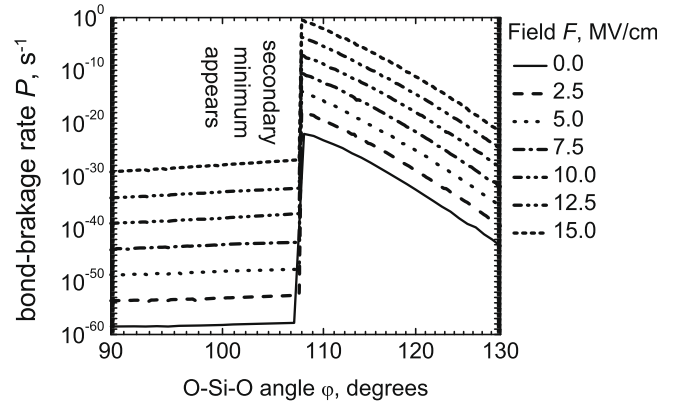


Fig. 3. Bond-breakage rate as a function of the O–Si–O angle  $\varphi$  calculated for various fields  $F$ .

#### 5. Statistical analysis

For the statistical analysis of bond-breakage rate deviations due to the fluctuations of O–Si–O angles we borrowed the probability density distribution of the O–Si–O angle,  $D_\varphi(\varphi)$ , from [5], represented in the inset of Fig. 5. The distribution function  $D_P$ , the mean value  $\langle P \rangle$  and the standard deviation  $\sigma_P$  of the variate  $P$  have been calculated as:

$$D_P(P, F) = D_\varphi(\varphi(P, F)) \left| \frac{d\varphi(P, F)}{dP} \right| \quad (9a)$$

$$\langle P \rangle = \int_0^\pi P(\varphi) D_\varphi(\varphi) d\varphi \quad (9b)$$

$$\sigma_P = \left( \int_0^\pi (P - \langle P \rangle)^2 D_\varphi(\varphi) d\varphi \right)^{1/2} \quad (9c)$$

Fig. 5 shows the mean value of the bond-breakage rate  $\langle P \rangle$  and its standard deviation  $\sigma_P$  as a function of the electric field  $F$ . As a reference, the nominal breakage rate  $P_n$  calculated for a fixed  $\varphi = 109.48^\circ$  (corresponding to the crystalline  $\alpha$ -quartz) is also plotted. One can see that for a wide range of the applied electric field,  $F = 5.0 \dots 10.0$  MV/cm, the mean value  $\langle P \rangle$  is more than five times higher than that calculated with  $\varphi = 109.48^\circ$ . Moreover, the standard deviation  $\sigma_P$  is comparable to  $P_n$  implying a quite wide span of variate  $P$ . Such a finding means that huge bond-breakage rates – realized with a small but still finite (nonzero) probability – may warrant the build-up of precursors for the formation of a percolation path. In fact, as it has been reported in the literature (e.g. [13]), while the trap cluster is being formed, new defects are most

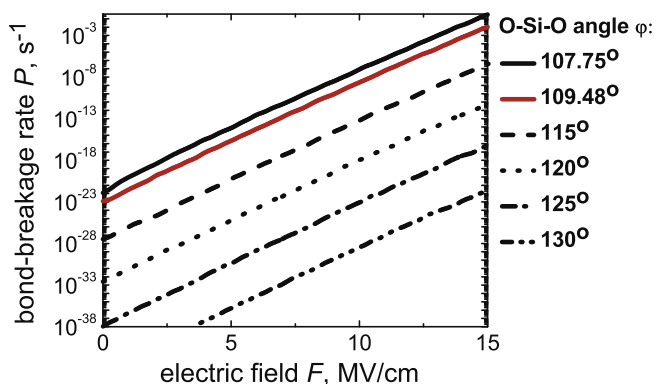


Fig. 4. Bond-breakage rate vs. the electric field  $F$  obtained for diverse angles  $\varphi$ .

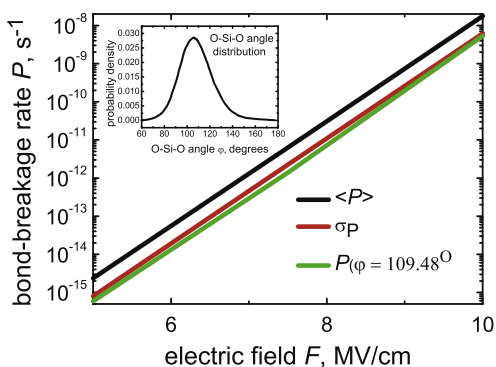


Fig. 5. The mean value, the standard deviation and the value calculated for  $\varphi = 109.48^\circ$  of bond-breakage rate. Inset: O–Si–O angle distribution borrowed from [5].

probably created in the vicinity of the pre-existed ones and thus the spot with the highest  $P$  acts as a precursor for the formation of a percolation path.

The family of density functions calculated for several values of the electric field  $F$  is depicted in Fig. 6. An important peculiarity of the probability density  $D_P$  is the invariance of its (linear) shape with respect to the applied electric field. In fact, an accelerating of  $F$  leads to the parallel shift of the curves towards higher  $P$  (in a log–log scale). Note that the normalization is guaranteed due to the trade-off between the exponential expansion of the spread towards higher rates and also the exponential reduction of the abso-

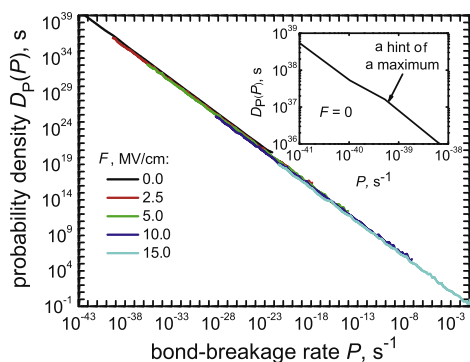


Fig. 6. The family of distribution function of the rate  $P$  calculated for various values of the applied electric field. Inset: a hint of a maximum revealed by the probability density obtained for  $F = 0$ .

lute values of  $D_P$ . This feature comes from the equidistance arrangement of dependencies  $P = P(\varphi)$  (calculated at a fixed step in  $F$ ) on a semi-log scale, see Fig. 4.

The distribution  $D_\varphi(\varphi)$  features the maximum at  $\varphi = 109.48^\circ$  and rapidly decays at both sides from this value. At the same time,  $P(\varphi)$  decreases (as well as  $|d\varphi/dP|$  in Eq. (9a)) with  $\varphi$  (starting from  $\varphi = \varphi_{cr}$ ) and therefore, in the range  $[\varphi_n; \varphi_{cr}]$  we have a superposition of two tendencies which may lead to the maximum being shifted with respect to the maximum of  $D_\varphi(\varphi)$  achieved at  $\varphi = \varphi_n$ . However,  $|d\varphi/dP|$  varies pretty fast with  $P$  and – being the predominant factor – inhibits contributions due to  $D_\varphi(\varphi)$ . As a result we see only a hint of a maximum represented in Fig. 6, inset (this example shows the fragment of the distribution for the zero field, i.e. curve  $D_P(P, F = 0)$ ).

As a consequence, this feature of  $D_P$  leads to a linear dependence of the bond-breakage rate on the electric field which has been also obtained for the case of a strongly fluctuating O–Si–O angle. Moreover, the standard deviation  $\sigma_P(F)$  reveals the same slope in the semi-log scale (Fig. 5) as  $\langle P \rangle(F)$ . These circumstances reflect the fact that the thermo-chemical model for the silicon–oxygen bond-breakage developed for crystalline silica is also applicable for amorphous material characterized by deviations in O–Si–O angle. In fact, the model demonstrates a linear decay of the logarithmic bond-breakage rate with the electric field. It treats the bond-breakage process in terms of chemical reactions with a certain activation energy and shows that this energy decreases proportionally to  $F$ . In our case the same result has been obtained, however under consideration of the fluctuating O–Si–O angle we substitute the nominal rate by the mean value and all the previous conclusions remain valid also in this case. To be more concrete, the logarithmic (mean) bond-breakage probability is being enlarged proportionally to the applied field.

## 6. Conclusions

Using the McPherson model for the Si–O bond rupture we analyzed the effect of O–Si–O bond angle  $\varphi$  variations on the breakage probability. While varying  $\varphi$  the potential profile is being transformed, i.e. the secondary minimum becomes deeper, which is accompanied by a growth of the separation barrier height. Hence, a trade-off between a lower barrier transparency and involvement of a larger number of energy levels for the Si ion tunneling between the primary and the secondary minima is typical for this situation. The secondary energetical minimum was shown to appear at  $\varphi_{cr} = 107.75^\circ$ .

The Si ion “finds” a way for bond-breakage corresponding to the highest probability and the direction featuring this maximal rate should be considered the bond-breakage pathway. While writing the “bond-breakage rate” we mean just this maximal value and distinguish this quantity and the nominal rate  $P_n$  calculated for the fixed  $\varphi = 109.48^\circ$ . We calculated the angle between this direction and the  $\text{SiO}_4$  tetrahedron symmetry axis as a function of the O–Si–O angle. For  $\varphi < 109.48^\circ$  (fixed value typical for crystalline silica) this direction is rotated with respect to the symmetry axis toward the deviated O ion, for  $\varphi = 109.48^\circ$  it coincides with the symmetry axis, being turned in the opposite side for higher  $\varphi$ .

Calculated – with a fixed step in the applied electric field  $F$  as a parameter – the dependencies of the bond-breakage rate  $P$  vs. O–Si–O angle are equidistantly spaced in a semi-log space. This means that the same activation bond-breakage nature is revealed in a wide range of angles  $\varphi$ . Such a concept is confirmed explicitly by a family of curves  $P = P(F)$ , demonstrating an exponential relation between the rate and the field.

Based on the O–Si–O angle distribution we evaluated the probability density  $D_P(P)$ , the mean value  $\langle P \rangle$  and the standard deviation

$\sigma_P$  of the statistically distributed variable  $P$ . The distribution function demonstrates the linear behavior while another peculiarity is that the electric field does not change the shape of the curves which are just shifted in parallel. The consequence of such a behavior is a similar log–lin slope for dependencies of the mean value, standard deviation and the nominal value of rate  $P$  vs. the electric field. This circumstance supports the thermo-chemical model (showing a linear increase of the logarithmic bond-breakage rate with increasing electric field) also for the case of strongly fluctuating O–Si–O bond angles.

In this case the mean value  $\langle P \rangle$  rather than the nominal rate  $P_n$  should be used to describe the rupture process. In a large range of electric fields, the mean rate  $\langle P \rangle$  is more than five times higher than the nominal rate  $P_n$ , while  $\sigma_P$  is comparable to  $P_n$ . Such a wide spread of the variable  $P$  means that an amorphous SiO<sub>2</sub> film contains spots (Si–O bond substantially weakened by a lattice distortion due to strongly deviated bond angles) with a rather high bond-breakage rate. Although the relative quantity of these spots is small, just these spots are predominately broken down during the electrical stress. Since the new defects are being prevalently formed in the vicinity of preexisting ones, such spots are very important because they act as grains for the initial stage of a percolation path formation.

## References

- [1] Mahapatra S, Saha D, Varghese D, Kumar PB. On the generation and recovery of interface traps in MOSFETs subjected to NBTI, FN and HCI stress. *IEEE Trans Electron Dev* 2006;ED-53(7):1583–92.
- [2] Kimura M, Koyama H. Mechanism of time-dependent oxide breakdown in thin thermally grown SiO<sub>2</sub> films. *J Appl Phys* 1999;85:7671–81.
- [3] McPherson JW. Extended Mie–Grüneisen molecular model for time dependent dielectric breakdown in silica detailing the critical roles of O–Si–O<sub>3</sub> tetragonal bonding, stretched bonds, hole capture, and hydrogen release. *J Appl Phys* 2006;99(8):083501.
- [4] McPherson JW. Quantum mechanical treatment of Si–O bond breakage in silica under time dependent dielectric breakdown. In: 45th Annual international reliability physics symposium IRPS-2007; 2007. p. 209–15.
- [5] Carré A, Horbach J, Ispas S, Kob W. New fitting scheme to obtain effective potential from Car–Parrinello molecular-dynamics simulations: application to silica. *Lett J Exp Front Phys* 2008;82(1):17001–10.
- [6] Alftan SV, Kuronen A, Kaski K. Realistic models for amorphous silica: a comparative study of different potentials. *Phys Rev B* 2003;68(7):073203-1.
- [7] Munetoh S, Motooka T, Morihuchi K, Shintani A. Interatomic potential for Si–O systems using Tersoff parameterization. *Comput Mater Sci* 2007;39(2):334–9.
- [8] Tucker MG, Keen DA, Dove MT, Trachenko K. Refinement of the Si–O–Si bond angle distribution in vitreous silica. *J Phys: Condens Mater* 2005;17(5):S67–75.
- [9] Helms CR, Poindexter EH. The silicon–silicon–dioxide system: its microstructure and imperfections. *Rep Prog Phys* 1994;57(7):791–852.
- [10] Vexler MI. A simple quantum model for the MOS structure in accumulation mode. *Solid-State Electron* 2003;47(8):1283.
- [11] Press WH, Teukolsky AA, Vetterling WT, Flannery BP. *Numerical recipes in C*. Cambridge University Press; 1997.
- [12] Cheung KP. Unifying the thermal–chemical and anode-hole-injection gate-oxide breakdown models. *Microelectron Reliab* 2001;41(2):193–9.
- [13] Bersuker G, Korin A, Fonseca L, Safonov A, Bagatur'yants A, Ruff HR. The role of localized states in the degradation of thin gate oxides. *Microelectron Eng* 2003;69(2–4):118–29.